ISSN 1070-3284, Russian Journal of Coordination Chemistry, 2014, Vol. 40, No. 12, pp. 925–931. © Pleiades Publishing, Ltd., 2014.

An Erbium-Organic Polymer Incorporating 2-(Hydroxyl)-6-Methylisonicotinic and Oxalate Coligand with 6^3 Topology[1]

A. Q. Tian[a, b], J. L. Chen[c], X. Feng[b, *], X. M. Lang[b], and L. Y. Wang[b, c]

[a] *Basic Courses Education Department, Henan Forestry Vocational College, Luoyang, 471002 P.R. China*

[b] *College of Chemistry and Chemical Engineering, Luoyang Normal University, Luoyang, 471022 P.R. China*

[c] *College of Chemistry and Pharmacy Engineering, Nanyang Normal University, Nanyang, 473601 P.R. China*

**e-mail: fengx@lynu.edu.cn*

Received June 2, 2014

Abstract—A new lanthanide–organic framework incorporating both substituted isonicotinic acid and oxalate coligand has been fabricated successfully through solvo-thermal reaction, namely, $\{[Er(\mu_2\text{-}H_2Minca)](\mu_2\text{-}C_2O_4 \cdot 2H_2O] \cdot 2H_2O\}_n$ (**I**) (H_3Minca = 2-(hydroxyl)-6-methyl-isonicotinic acid, $H_2C_2O_4$ = oxalate acid). Complex **I** exhibits two dimensional (2D) corrugated networks with a 6^3 topology, in which $\{LnO_8\}$ polyhedron units are alternately linked through carboxylate and oxalate oxygen atoms into the 2D sheet layer (CIF file CCDC no. 948026). Thermogravimetric and different thermal analysis measurements indicate that **I** displays high thermal stability. Complex **I** also shows characteristic *f–f* transition luminescence emission in NIR region.

DOI: 10.1134/S1070328414120136

INTRODUCTION

Over the last decades, the construction of lanthanide carboxylate based metal-organic frameworks (Ln-MOFs) has been a field of rapid growth not only for their intriguing architectures and topologies but also for their applications in areas of catalysis, sorption, separation, luminescence, magnetism, non-linear optical property, etc. [1, 2], because of their special chemical and physical properties arising from the unique spectroscopic and 4*f* electronic. A large part of these studies is concerned with homo- and heteropolymetallic compounds obtained using compartmental polydentate ligands and is motivated by optical or magnetic properties or biological interest, and a variety of multicarboxylate pyridimine/imidazoline/pyridine-based ligands have been extensively employed for exhibiting various coordination fashions with magnetic and luminescent properties, and so on [3, 4]. At the same time, oxalate, as the smallest dicarboxylate, is rigid and coplanar, has a small stereo effect which is beneficial for constructing MOFs [5]. Meanwhile, oxalate has been proved to be a good candidate for pillar ligand due to its various bridging abilities and strong coordination tendency to generate 1D to 3D moderately robust networks, exhibiting tunable ferro or antiferro-magnetic exchanges [6]. The oxalate within lanthanide carboxylate system can reduce or eliminate water molecules from the coordination sphere of the central ions, hence increasing the luminescent intensity and lifetime of the materials [7]. The introduction the electron donating species (e.g., methyl group) to isonicotinic acid is expected to enhance the coordination ability of ligand and facilitate the electron transfer within the compounds [6]. As a continuation of our previous investigation [8], and in order to better understand the coordinating behavior and role of the oxalate in the self–assembly processes and the properties in these systems, a new erbium-organic framework has been isolated through the lanthanide salts reaction with isonicotinic acid derivative under hydrothermal synthesis condition.

EXPERIMENTAL

Materials and physical measurements. All reagents used in the syntheses were of analytical grade and used as received. Elemental analyses for carbon, hydrogen and nitrogen atoms were performed on a Vario EL III elemental analyzer. The infrared spectra (4000–400 cm^{-1}) were recorded by using KBr pellet on an Avatar TM 360 E.S.P. IR spectrometer. Thermogravimetric analyses (TGA) were performed under atmosphere with a heating rate of 10°C/min^{-1} using TGA/SDTA851e. The powder X-ray diffraction (PXRD) patterns were measured using a Bruker D8 Advance powder diffractometer at 40 kV, 40 mA for CuK_α radiation (λ = 1.5418 Å) with a scan speed of 0.2 s/step and a step size of 0.02 (2θ). Luminescence spectra of the complexes in solid state were carried out on a Cary Eclipse fluorescence spectrophotometer.

[1] The article is published in the original.

Table 1. Crystallographic data and experimental details for compound **I**

Parameter	Value
Formula weight	465.46
Temperature, K	293(2)
Crystal system	Triclinic
Space group	*P*
a, Å	7.3640(5)
b, Å	8.5482(6)
c, Å	10.6487(7)
α, deg	106.6640(10)
β, deg	102.2210(10)
γ, deg	94.4670(10)
Volume, Å^3; *Z*	620.71(7); 2
ρ_{calcd}, g/cm^3	2.469
Absorption coefficient, mm^{-1}	6.817
Index ranges	$-7 \le h \le 9$, $-11 \le k \le 11$, $-13 \le l \le 11$
F(000)	442
θ Range for data collection, deg	2.06–27.50
Independent reflections	2744
Observed reflections	3787
Refinement method	Full-matrix least-squares on F^2
Data/restraints/parameters	2744/12/200
Goodness-of-fit on F^2	0.998
R index ($I > 2\sigma(I)$)	R_1 =0.0202, wR_2 = 0.0513
R index (all data)	R_1 = 0.0211, wR_2 = 0.0520
Largest diff. peak/hole, *e* Å^{-3}	0.876/−1.594

Synthesis of $\{[Er(\mu_2\text{-}H_2Minca)](\mu_2\text{-}C_2O_4) \cdot 2H_2O] \cdot 2H_2O\}_n$ (I). Organic ligand H_3Minca (0.039 g, 0.2 mmol) and sodium oxalate dihydrate (0.029 g, 0.2 mmol) in a solution of water–DMF (V/V = 2.0, 10 mL) were mixed with an aqueous solution (10 mL) of 0.1 mmol, (0.0439 g) $Er(NO_3)_3 \cdot 6H_2O$. After stirring for 20 min in air, the pH value was adjusted to 5.5 with nitric acid, and the mixture was placed into 25 mL Teflon-lined autoclave under autogenous pressure being heated at 150°C for 72 h, then the autoclave was cooled over a period of 24 h at a rate 5°C/h. After filtration, the product was washed with distilled water and then dried, colorless crystals of **I** were obtained suitable for X-ray diffraction analysis. For **I**, the yield was 0.0144 g (34%) based on Er.

For $C_9H_{10}NO_9Er$

anal. calcd., %:	C, 25.34;	H, 2.36;	N, 3.28.
Found, %:	C, 25.26;	H, 2.49;	N, 3.21.

IR (KBr; ν, cm^{-1}): 3402 br, 3342 s, 2946 s, 1621 s, 1532 s, 1413 m, 1374 s, 1087 s, 929 v.s, 747 m, 668 s, 457 m.

X-ray structure determination. A single crystal of the title complex (0.25 × 0.21 × 0.17 mm) was mounted on a Bruker SMART APEX II CCD diffractometer equipped with a graphite-monochromatized MoK_α radiation (λ = 0.71073 Å) by using a φ/ω scan mode at room temperature in the range of $2.35^o \le \theta \le 25.49°$. Corrections for *Lp* factors were applied and all non-hydrogen atoms were refined with anisotropic thermal parameters. The structure was solved by direct methods with SHELXS-97 [9]. The hydrogen atoms were assigned with common isotropic displacement factors and included in the final refinement by use of geometrical restrains. A full-matrix least-squares refinement on F^2 was carried out using SHELXL-97 [10]. The final R_1 = 0.0211, wR_2 = 0.0520, ($w = 1/[\sigma^2(F_o^2) + (0.0296P^2) + 1.5268P]$, where $P = (F_o^2 + 2F_c^2/3)$, S = 0.998, $(\Delta\rho)_{max}$ = 0.876 and $(\Delta\rho)_{min}$ = −1.594 *e*/Å^3. Crystallographic and experimental details are summarized in Table 1. The selected bond lengths and bond angles are listed in Table 2.

Supplementary material for structure **I** has been deposited with the Cambridge Crystallographic Data Centre (no. 948026; deposit@ccdc.cam.ac.uk or http://www.ccdc.cam.ac.uk).

RESULTS AND DISCUSSION

In the IR spectra of compound **I**, the presence of the broad and strong characteristic stretches in frequency region of 3200–3450 cm^{-1} are assigned to the characteristic peaks of OH vibration of free water molecules. The strong vibrations appeared around 1640 and 1390 cm^{-1}

Table 2. Selected bond lengths (Å) and angles (deg) for complex **I***

Bond	*d*, Å	Bond	*d*, Å	Bond	*d*, Å
Er(1)–O(2)$^{\#1}$	2.250(3)	Er(1)–O(1*w*)	2.324(3)	Er(1)–O(5)$^{\#3}$	2.390(2)
Er(1)–O(1)	2.302(2)	Er(1)–O(2*w*)	2.339(3)	Er(1)–O(6)	2.440(3)
Er(1)–O(4)	2.322(3)	Er(1)–O(7)$^{\#2}$	2.370(3)		
Angle	ω, deg	Angle	ω, deg	Angle	ω, deg
O(2)$^{\#1}$Er(1)O(1)	85.00(10)	O(1)Er(1)O(1*w*)	149.51(10)	O(4)Er(1)O(2*w*)	146.74(10)
O(2)$^{\#1}$Er(1)O(4)	100.58(10)	O(4)Er(1)O(1*w*)	139.06(9)	O(1*w*)Er(1)O(2*w*)	74.19(10)
O(1)Er(1)O(4)	71.37(9)	O(2)$^{\#1}$Er(1)O(2*w*)	78.45(10)	O(2)$^{\#1}$Er(1)O(7)$^{\#2}$	149.46(10)
O(2)$^{\#1}$Er(1)O(1*w*)	86.38(10)	O(1)Er(1)O(2*w*)	75.45(10)	O(1)Er(1)O(7)$^{\#2}$	75.03(9)
O(4)Er(1)O(7)$^{\#2}$	94.72(10)	O(1)Er(1)O(5)$^{\#3}$	130.31(9)	O(7)$^{\#2}$Er(1)O(5)$^{\#3}$	136.17(9)
O(1*w*)Er(1)O(7)$^{\#2}$	99.15(10)	O(4)Er(1)O(5)$^{\#3}$	68.94(9)	O(2)$^{\#}$Er(1)O(6)	143.34(10)
O(2*w*)Er(1)O(7)$^{\#2}$	74.35(10)	O(1*w*)Er(1)O(5)$^{\#3}$	74.51(9)	O(1)Er(1)O(6)	124.46(10)
O(1*w*)Er(1)O(6)	77.18(10)	C(1)O(1)Er(1)	131.4(2)	C(9)O(6)Er(1)	118.6(2)
O(2*w*)Er(1)O(6)	126.24(10)	C(1)O(2)Er(1)$^{\#1}$	143.4(3)	C(9)O(7)Er(1)$^{\#2}$	121.1(2)
O(7)$^{\#2}$Er(1)O(6)	66.53(9)	C(8)O(4)Er(1)	118.8(2)	O(4)Er(1)O(6)	73.49(10)
O(5)$^{\#3}$Er(1)O(6)	69.81(9)	C(8)O(5)Er(1)$^{\#3}$	115.9(2)		
O(2)$^{\#1}$Er(1)O(5)$^{\#3}$	74.31(9)	O(2*w*)Er(1)O(5)$^{\#3}$	139.34(9)		

* Symmetry codes: $^{\#1}$ $-x+1, -y+1, -z+1$; $^{\#2}$ $-x, -y, -z+1$; $^{\#3}$ $-x, -y+1, -z+1$.

correspond to the asymmetric and symmetric stretching vibrations of the carboxylic group [11]. The strong absorption at ~2950 cm^{-1} indicates the existence of methyl group. In IR spectra, the peaks at ~1590 cm^{-1} are assigned to the coordinated $C_2O_4^{2-}$ anions [12]. The absence of strong bands ranging from 1690 to 1710 cm^{-1} indicates that the completely deprotonation of carboxylic groups of pyridine carboxylic tectonic. The binuclear units linked by H_3Minca and oxalate ligands in compound **I** are illustrated in Scheme:

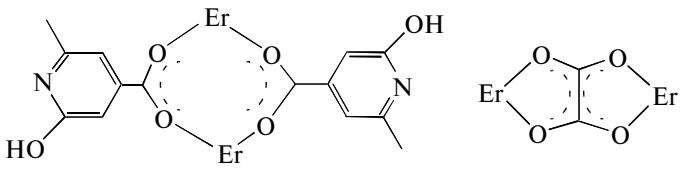

(a) (b)

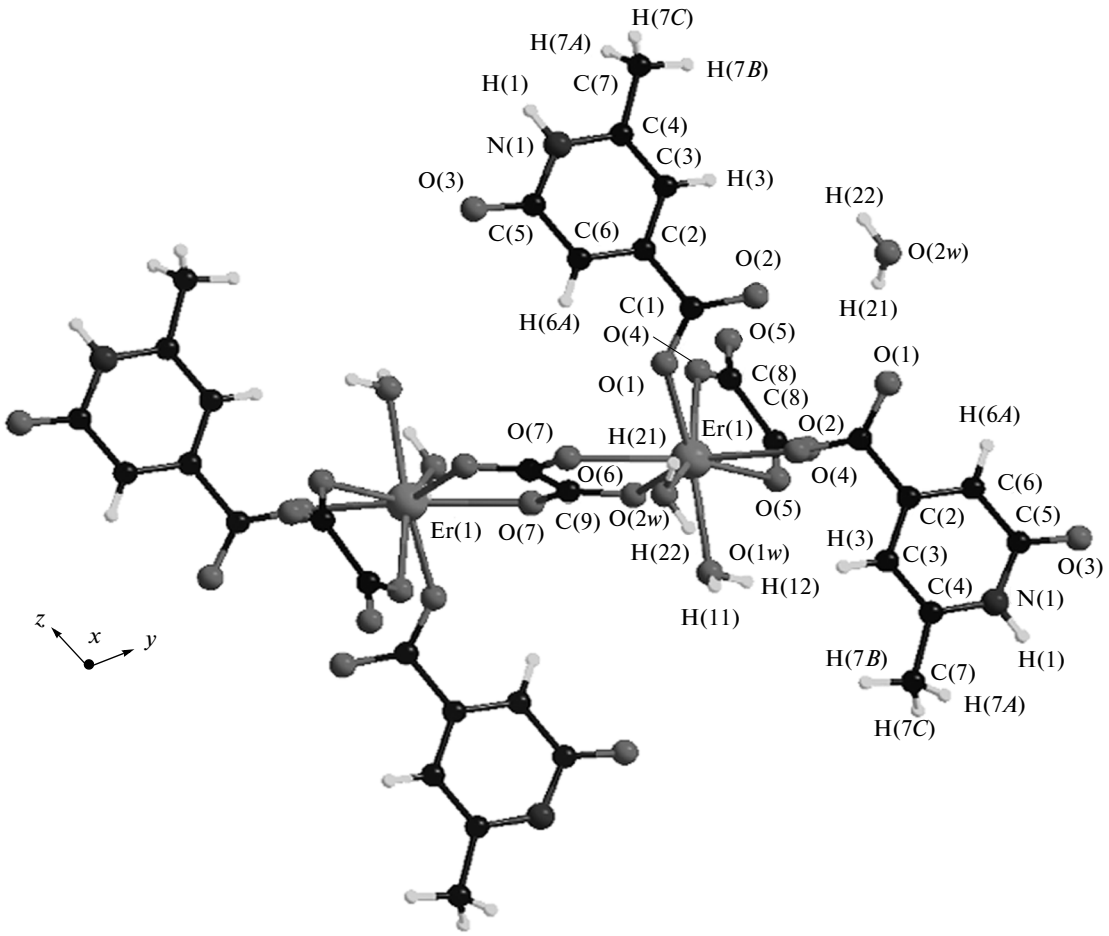

Fig. 1. The different coordination environments of Er^{3+} ions in symmetric unit of **I**.

Single X-ray diffraction analysis reveals that complex **I** is crystallizing in triclinic system with space group of $P\bar{1}$. They are all found to be lanthanide-organic polymers based on discrete binuclear lanthanide carboxylate aggregates and one free water molecule. As illustrated in Fig. 1, the asymmetric unit of **I** is composed of an eight-coordinated Er^{3+} cation, two H_3Minca ligands, two oxalate and one coordinated waters, as well as one uncoordination water molecule. In this unit, each H_3Minca ligand provides two O atoms from the one carboxylic group to connect two adjacent Er^{3+} ions (see Scheme). The oxalate ligand acts as bidentate and chelating ligand linking to two metal nodes. The dihedral angle between the neighboring oxalate ligands sharing the common erbium(III) ion is 73.02°. Interestingly, the pyridine-N and hydroxyl-O do not coordinate to central ion. The remaining two sites were occupied by oxygen atom of water molecules, completing the distorted dodecahedral coordination. Bond Er–O distances involving the central ion (2.250(3) and 2.440(3) Å) are closely similar to those observed in several related lanthanide species [13].

The H_3Minca has been deprotonated for carboxyl groups, but an H atom was added to pyridine N bearing one positive charge, and the hydroxyl group has been deprotonated, so it is denoted as H_2Minca^-, correspondingly. All H_2Minca-anion ligands have the same coordination mode with dangling lateral methyl arms, employing carboxylic group doubly connecting two Er^{3+} ions to form a binuclear unit with the shortest distance Er(III)···Er (III) of 5.109 Å. The two carboxylate connected two Er^{3+} ions, resulting in an eight remembered chair-like ring. There is a unique bridging oxalate ligand chelating the two adjacent Er^{3+} ions in binuclear unit via its oxygen atoms, connecting these eight remembered rings, giving rise to a 1D ribbon infinite chain along the *xz* plane, as displayed in Fig 2a. At the same time, the two neighboring Er^{3+} ions are al-

so connected via oxalate oxygen to form a Er_2 diunclear unit with the Er···Er separation of 6.245 Å. These binuclear segments are further grafted on to the 1D infinite ribbon zigzag chain array along the crystallographic *z* axis (Fig. 2b). Moreover, the carboxylate from next H_3Minca ligand acts as a linker, alternately connecting these 1D chains into an interesting corrugated 2D lamellar sheet along *xy* plane, as displayed in Fig. 3. The individual nets are undulated and sinusoidal in nature [14].

In this sheet, six Er^{3+} ions were alternately connected by four oxalate and two carboxylates from H_3Minca to form a six remembered ring. This is neither similar to other reported transition metal complexes, in which the central ions are connected through ambient oxalate ligands to form honeycomb homometallic layers [15], nor it is different from the lanthanide complexes containing oxalatophosphonates, in which six Ln^{3+} ions were linked through six oxalate anions into a netlike $\{Ln(C_2O_4)_n\}$ 24-member ring in a layer [16]. However, when the binuclear Er_2 unit doubly connected through carboxylic group is regarded as a three connected node, the whole structure can be described as a uninodal 3-connected corrugated network, with 3, 6 hcb topology [17], and the point symbol is 6^3, as shown in Fig. 4.

Carefully inspection of the structure reveals the adjacent 2D coordination networks are further interlinked by hydrogen bonding interactions. These layers are further stacked together and extended into 3D supramolecular edifice through the strong interlayer hydrogen interactions between carboxylic group and free water oxygen atoms from the adjacent 2D corrugated sheets, such as (O(1*w*)–H(11)...O(3)$^{\#4}$, O···O 2.752(4) Å, angle O···H–O 123.8°), and the hydrogen bonding parameters are listed in Table 3 for details.

The powder XRD patterns of compound **I** shows strong peaks where 2 theta are 9.6, 13.7, 16.2, 18.8, 26.3, 32.9 degrees, respectively, which are well matched with the simulation ones based on single-crystal data analysis, and this indicates the bulk sample of I obtained is in a pure phase. The thermal stability of I was also explored by the thermogravimetric (TG) and different thermal analysis (DTA) (Fig. 5). The TGA diagram of **I** exhibits an initial mass loss of 13% corresponding to start with the departure of one lattice water as well as two coordinated water molecules in the temperature about 220°C, and the decomposition of **I** begins above 300°C, which is attributed to the release of the oxalate groups 17.3% (calcd. 18.4%). Compound **I** begins to decompose upon further heating and underwent a rapid and significant weight loss of 32.8% beyond the temperature of 450°C, correspond-

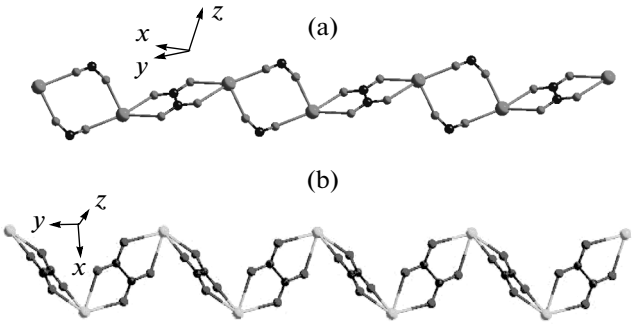

Fig. 2. Diamond illustration of the 1D ribbon chain connected by oxalate in **I** along *y* (a) and *x* axises (b). The H atoms and free waters are not included for clarity.

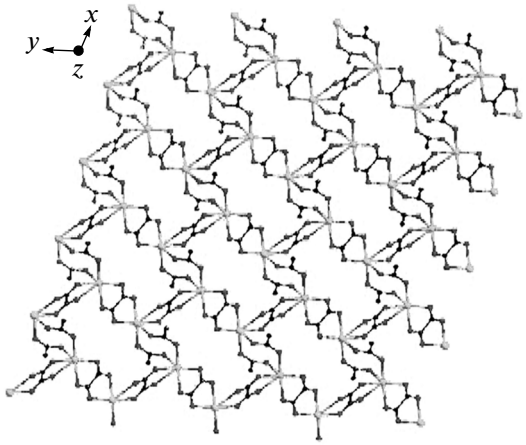

Fig. 3. Projective view of 2D corrugated layer consisting of 1D zigzag chain along *xy* plane.

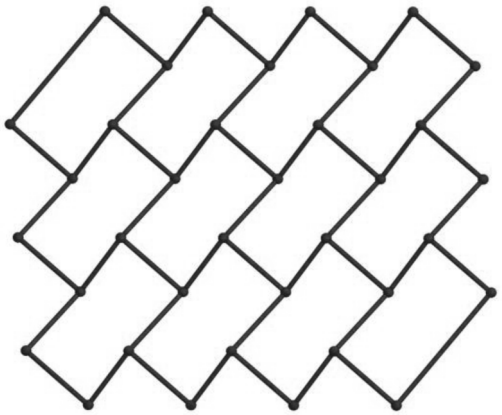

Fig. 4. Illustration of 3-connected hcb topological network in **I**.

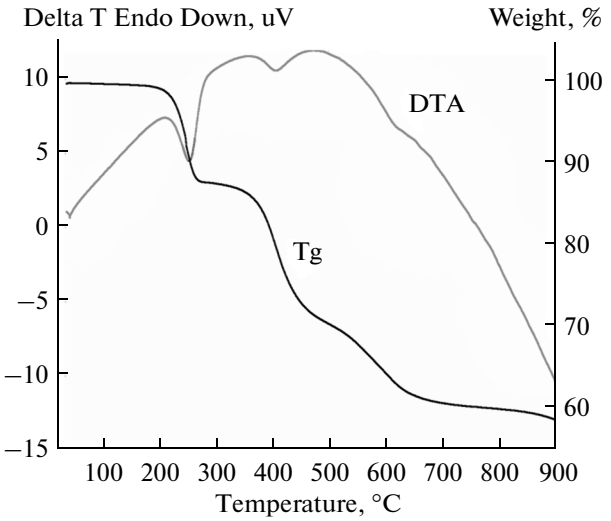

Fig. 5. TG–DTA curves for compound **I**.

ing to the destruction of the H_2Minca organic ligands (calcd. 33.6%).

Taking into accounting the promising luminescent properties of erbium complexes, photoluminescence measurements of the ethanol suspension samples (~0.001 mol/L) of I were investigated at room temperature. As illuminated in Fig. 6a, it shows excitation luminescence maximum at wavelength of 412 nm, which is attributed to $\pi \rightarrow \pi^*$ and/or $n \rightarrow \pi^*$ transition, upon photoexcitation with 380 nm, the title complex exhibited emission spectra in the region from 1520 to 1660 nm (in near infrared region) with the maximum wavelength of 1538 nm (Fig. 6b). Thus, the emission observed in the complexes is tentatively assigned to the $^4I_{3/2} \rightarrow {}^4I_{15/2}$ fluorescence of Er^{3+} ion [18].

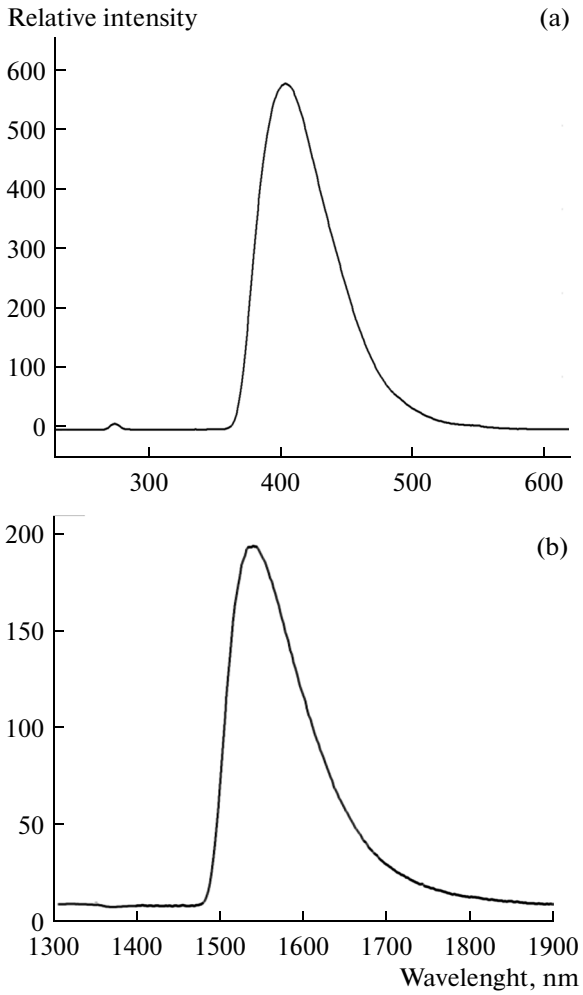

Fig. 6. The liquid-state excitation (a) and emission (b) spectra of sample **I** in methanol suspension at room temperature in the near-IR region.

Table 3. Geometric parameters of hydrogen bonds for complex **I***

D–H···A	Distance, Å			Angle DHA, deg
	D–H	H···A	D···A	
O(1*w*)–H(11)···O(3)$^{\#4}$	0.84	2.19	2.752(4)	124
O(1*w*)–H(12)···O(3)$^{\#5}$	0.84	2.02	2.746(4)	145
O(2*w*)–H(22)···O(3*w*)	0.84	1.93	2.735(8)	159
O(2*w*)–H(22)···O(3*w*)	0.84	1.95	2.492(17)	121
N(1)–H(1)···O(5)$^{\#6}$	0.88	2.14	3.006(4)	167

* Symmetry transformations used to generate equivalent atoms: $^{\#4}$ $-x+1, -y, -z+1$; $^{\#5}$ $x-1, y, z-1$; $^{\#6}$ $-x+1, -y+1, -z+2$ (#1, #2, #3 see Table 2).

ACKNOWLEDGMENTS

This work was supported by the National Natural Science Foundation of China (nos. 21273101 and 21271098), Foundation of the Program for Backbone Teachers in Universities of Henan Province (no. 2012GGJS158), Program for Science & Technology Innovation Talents in Universities of Henan Province (2014HASTIT014), and Tackle Key Problem of Science and Technology Project of Henan Province, China (no. 142102310483).

REFERENCES

1. Rosi, N.L., Echert, J., Eddaoudi, M., et al., *Science*, 2003, vol. 300, no. 1127, p. 5622.

2. Rao, C.N., Natarajan, S., and Vaidhyanathan, R., *Angew. Chem. Int. Ed.*, 2004, vol. 43, p. 1466.
3. An, H.Y., Zhang, H., Chen, Z.F., et al., *Dalton Trans.*, 2012, vol. 41, p. 8390.
4. Feng, X., Li, S.H., Wang L.Y., et al., *CrystEngComm*, 2012, vol. 14, p. 3684.
5. Feng, X., Ling, X.L., Liu, L., et al., *Dalton Trans.*, 2013, vol. 42, no. 28, p. 10292.
6. Feng, X., Wang, J.G., Liu, B., et al., *Cryst. Growth Des.* 2012, vol. 2, no. 2, p. 927.
7. Rashid, S., Turner, S.S., Pevelen, D., et al., *Inorg. Chem.*, 2001, vol. 40, no. 20, p. 5304.
8. Feng, X., Zhao, J.S., Liu, B., et al., *Cryst. Growth Des.*, 2010, vol. 10, no. 3 p. 1399.
9. Sheldrick, G.M., *SHELXS-97, Program for the Solution of Crystal Structure*, Göttingen (Germany) Univ. of Göttingen, 1997.
10. Sheldrick, G.M., *SHELXL-97, Program for the Crystal Structure Refinement*, Göttingen (Germany): Univ. of Göttingen, 1997.
11. Cheng, A.L., Ma, Y., Zhang, J.Y., and Gao, E.Q., *Dalton Trans.*, 2008, p. 1993.
12. Nakamoto, K., *Infrared and Raman Spectra of Inorganic and Coordination Compounds*, New York: Interscience-Wiley, 1986.
13. Liu, M.S., Yu Q.Y., Cai Y.P., et al., *Cryst. Growth Des.,* 2008, vol. 8, no. 11, p. 4083.
14. Feng, X., Zhao, J.-S., Wang L.Y., et al., *Inorg. Chem. Commun.*, 2009, vol. 10, no. 5, p. 388.
15. Yang, Z.Y., *Synth. React. Inorg. Met.-Org. Chem.*, 2002, vol. 32, no. 5, p. 903.
16. Li, X.F., Liu, T.F., Lin, Q.P., and Cao, R., *Cryst. Growth Des.*, 2010, vol. 10, no. 2, p. 608.
17. Qin, D.D., Yang, Z.Y., and Qin, G.F., *Spectrochim. Acta, A*, 2009, vol. 74, no. 2, p. 415.
18. Kornienko, A., Banerjee, S., Kumar, G.A., et al., *J. Am. Chem. Soc.*, 2005, vol. 127, no. 40, p. 14008.